Sensitivity Analysis of Helical Tube Geometric Parameters for Density Wave Oscillation Using MARS-KS Code

Seunghwan Oh [a], Doh Hyeon Kim [a], Junha Hwang [a], Semin Joo [a], Jeong Ik Lee [a*]
[a]*Nuclear & Quantum Engr. Korea Advanced Institue of Science and Technology (KAIST), 291 Daehak-ro, Yuseong-gu, Daejeon, Republic of Korea*

Keywords : Small modular reactor, Helical steam generator, Density wave oscillation, MARS-KS code

1. Introduction

Globally, advanced reactor developers are focusing on minimizing the reactor size to facilitate modular construction. A modular configuration simplifies installation and maintenance, and lowers construction costs. To achieve these goals, a helical steam generator (HSG) is being considered as a viable option.

However, in designing HSGs, it is crucial to address two-phase flow instabilities, such as density wave oscillation (DWO). The DWO mechanism involves delays and multiple feedback loops related to pressure drop, inlet flow rate, and void fraction [1]. At high void fractions, even small changes in inlet velocity can cause large fluctuations in two-phase friction pressure drop due to variations in density and flow, with these fluctuations propagating slowly and potentially destabilizing the system, leading to mechanical vibrations, system control failures, and thermal fatigue [2, 3].

Since an HSG is composed of tube bundles arranged in multiple layers, the geometrical values can vary across layers. It is essential to understand the sensitivity of DWO to these geometric parameters during the design process. These parameters include tube length, tube diameter, helical diameter, and helix angle (Fig. 1). Although experimental studies under different helical tube geometric conditions conducted by Papini [4], Wang [5], Shen [6], it is difficult to understand the single sensitivity of each parameter because the values of the parameters mentioned just before are all different.

2. Methods

In this section, the modeling of parallel helical tubes using the MARS-KS code is thoroughly explained, and summaries of the simulation cases and the thermal-hydraulic model are provided.

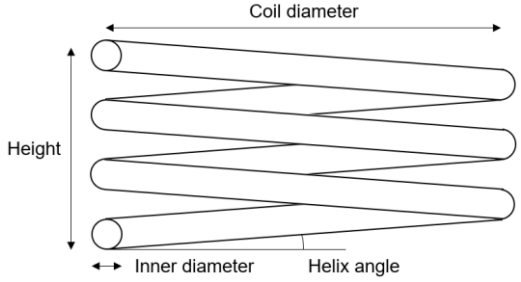

Fig. 1. Geometric parameters of the helical tube

2.1 Parallel Helical Tubes Modeling

MARS-KS V2.0 code is utilized to examine DWO. Fig. 2 shows the nodalization of parallel helical tubes. The fluid enters the problem domain with constant sub-cooling from a time dependent volume (TMDPVOL 100), and the inlet flow rate is determined using a time dependent junction (TMDPJUN 101). The helical tubes are modeled as inclined straight pipes (PIPE 10, 20) in MARS-KS code. The thermal-hydraulic model option for helical tubes is applied. The inlet and outlet of the pipes are linked to the inlet header (BRANCH 102) and the outlet header (BRANCH 103), respectively. The boundary for the outlet pressure is set by TMDPVOL 105. A uniform heat flux boundary condition is applied. The tube inlet throttle is modeled by assigning the energy loss coefficient of the junction connecting BRANCH 102 with PIPE 10 and 20. The method to determine instability is based on the previous research [7].

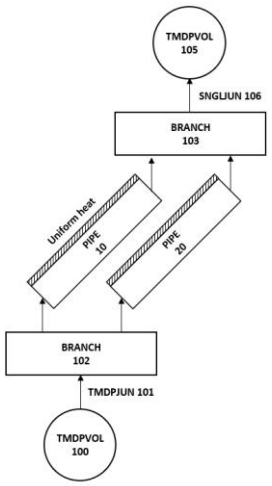

Fig. 2. Examples of parallel helical tubes nodalization

2.2 Thermal-hydraulic Correlations for Helical tubes in MARS-KS Code

The MARS-KS code is a system code developed for the safety evaluation of pressurized water reactors and heavy water reactors during licensing reviews by nuclear regulators [8]. It consists of governing and constitutive equations, with the latter being regularly updated to incorporate newly developed components and systems.

Among these updates is the inclusion of a heat transfer correlation for helical tubes. However, the MARS-KS code does not originally include correlations for pressure drop calculations in helical tubes. In this study, a modified version of the MARS-KS code was developed to incorporate pressure drop correlations for helical tubes. The Ito correlation [9] was applied for modeling single-phase flow, while the two-phase flow was modeled using the correlation developed by Colombo et al. [10], which was formulated using experimental data from studies by Santini et al. [11] and Zhao et al. [12]. Tables I and II summarize the heat transfer correlations and the pressure drop correlations for the modified MARS-KS code.

Table I: Heat transfer correlation

Single-phase turbulent
(Mori-Nakayama correlation)

$$h_{mn} = 0.03846\frac{k_k}{d}Re_k^{0.8}\frac{Pr}{\left(Pr_k^{\frac{2}{3}}-0.074\right)}\left(\frac{d}{D}\right)^{\frac{1}{10}}\left[1+\frac{0.061}{\left[Re_k\left(\frac{d}{D}\right)^2\right]^{\frac{1}{5}}}\right] \quad (1)$$

Nucleate boiling (Chen correlation)

$$q'' = h_{mn}(T_w - T_{sat})F + h_{mic}(T_w - T_{sat})S \quad (2)$$

$$h_{mic} = 0.00122\left(\frac{k_f^{0.79}C_{pf}^{0.45}\rho_f^{0.49}}{\sigma^{0.5}\mu_f^{0.29}h_{fg}^{0.24}\rho_g^{0.24}}\right)\Delta T_w^{0.24}\Delta P^{0.75}$$

$$S = \begin{cases} \left(1+0.12Re_{tp}^{1.14}\right)^{-1} & \left(Re_{tp} < 32.5\right) \\ \left(1+0.42Re_{tp}^{0.78}\right)^{-1} & \left(32.5 \le Re_{tp} < 70\right) \\ 0.0797 & \left(Re_{tp} \ge 70\right) \end{cases}$$

$$Re_{tp} = 10^{-4}Re_f F^{1.25}$$

Saturated nucleate boiling

$$F = 2.35\left(\chi_{tt}^{-1}+0.213\right)^{0.736}$$

Subcooled nucleate boiling

$$F' = \begin{cases} F - 0.2\left(T_{sat}-T_f\right)(F-1) \\ \left(T_{sat} > T_f \ge T_{sat}-5\right) \\ 1 \ \left(T_f < T_{sat}-5\right) \end{cases}$$

Transition boiling ($0.99 \le \alpha \le 0.999$)

$$q''_{TB} = q''_{NB}a_f + h_{mn}(T_w - T_g)(1-a_f)$$
$$a_f = 1.0 - \frac{\alpha - 0.99}{0.009} \quad (3)$$

Table II. Pressure drop correlation

Single-phase flow (Ito correlation)

$$f\left(\frac{D}{d}\right)^{\frac{1}{2}} = 0.029 + 0.304\left[Re\left(\frac{d}{D}\right)^2\right]^{-0.25} \quad (4)$$

Two-phase flow (Colombo correlation)

$$\emptyset_l^2 = 0.0986\left(1+\frac{20}{X_{tt}}+\frac{1}{X_{tt}^2}\right)De_l^{0.19}\left(\frac{\rho_m}{\rho_l}\right)^{-0.4} \quad (5)$$

$$De_l = \frac{G(1-x)d}{\mu_l}\sqrt{\frac{d}{D}} \quad \rho_m = \left(\frac{x}{\rho_g}+\frac{1-x}{\rho_f}\right)^{-1}$$

$$\Delta P_l = \frac{f_l G^2(1-x)^2 L}{2\rho_l d} \quad f: Ito\ cor \quad \Delta P_{tp} = \Delta P_l \emptyset_l^2$$

2.3 Simulation cases

Table III. Simulation cases

Case	Ref.	1	2	3	4
$d_i\ (mm)$	12	9	15	12	12
$L\ (m)$	25	25	25	15	35
δ	50	50	50	50	50
$\theta\ (°)$	8	8	8	8	8

Case	5	6	7	8
$d_i\ (mm)$	12	12	12	12
$L\ (m)$	25	25	25	25
δ	25	100	50	50
$\theta\ (°)$	8	8	16	24

d_i: Tube inner diameter L: Length δ: Curvature ratio (Helical diameter/Tube inner diameter) θ: Helix angle

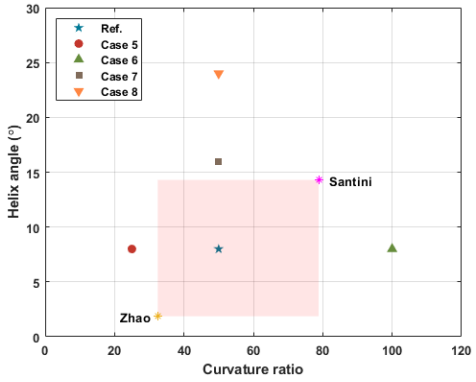

Fig. 3. Range of geometric conditions of each case

In this study, the reference tube was determined based on the public source [13, 14] of the helical steam generator of the SMART reactor developed by KAERI. Cases 1 and 2 analyze the sensitivity to tube inner diameter, Cases 3 and 4 to length, Cases 5 and 6 to curvature ratio, Cases 7 and 8 to helix angle. Although there are cases that exceed the dimensions of the experimental facility used for developing the Colombo correlation (Fig. 3), geometric parameter values were set over a wide range to analyze the overall sensitivity anyway. Cases 1 to 4 have the same curvature ratio and

helix angle as the reference, so they are omitted from Fig. 3. All cases were performed under the conditions of $G = 500kg/(m^2s)$, $P_{out} = 5MPa$. Therefore, in cases 1 and 2, the tube inner diameter is different, so the flow rate will become different.

2.4 Stability map

Once the fluid, tube geometry, and operating pressure are defined, it can identify stable and unstable regions within a three-dimensional space characterized by flow rate, heat power, and inlet subcooling. This space can be simplified into a two-dimensional plot using dimensionless numbers, which results in what is known as a stability map. The stability map developed by Ishii and Zuber [15] is the most widely used (see Eq. (6) and Eq. (7)). In this map, the stable region is represented on the left side of the boundary line, while the unstable region is on the right. Additionally, in the stability map, the diagonal line representing constant equilibrium quality corresponds to Eq. (8). To create a stability map, it is crucial to determine the instability threshold, which can be derived from experimental data or simulations across various operating conditions.

$$N_{pch} = \frac{Q}{\dot{m}h_{fg}}\frac{\rho_{fg}}{\rho_g} \tag{6}$$

$$N_{sub} = \frac{\Delta h_{in}}{h_{fg}}\frac{\rho_{fg}}{\rho_g} \tag{7}$$

$$N_{sub} = N_{pch} - x_e\frac{\rho_{fg}}{\rho_g} \tag{8}$$

3. Results

Fig. 4. shows the node sensitivity of inclined pipes under reference conditions. Based on these results 80 nodes were used for the simulation cases. Fig. 5 to Fig. 8 present sensitivity to each parameter. It was confirmed that the onset of DWO boundary conditions changed with respect to the tube inner diameter and length. In contrast, the occurrence of DWO was not sensitive to the curvature ratio and helix angle.

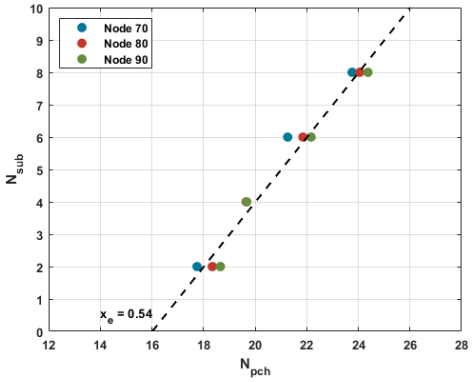

Fig. 4. Node sensitivity (Reference)

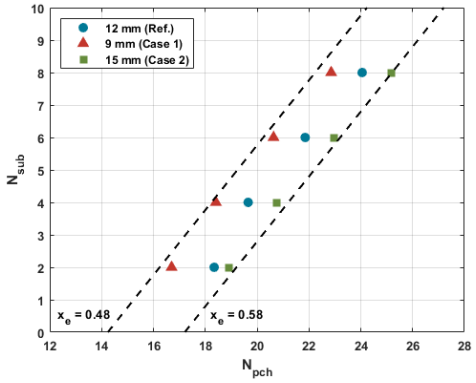

Fig. 5. Sensitivity to inner diameter (Cases 1 and 2)

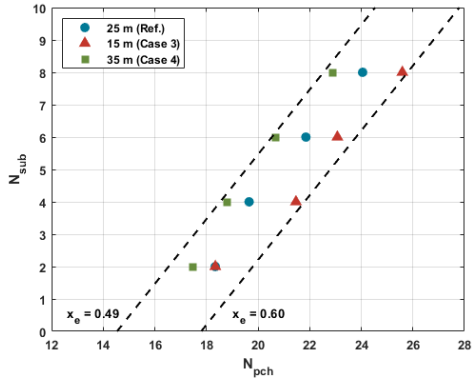

Fig. 6. Sensitivity to length (Cases 3 and 4)

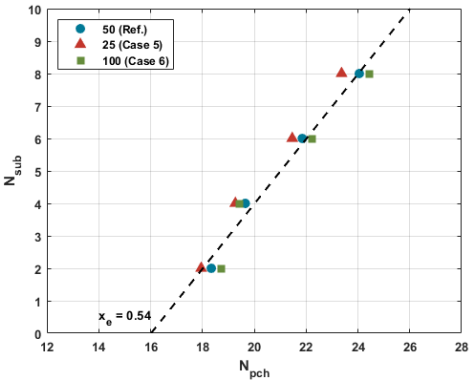

Fig. 7. Sensitivity to curvature ratio (Cases 5 and 6)

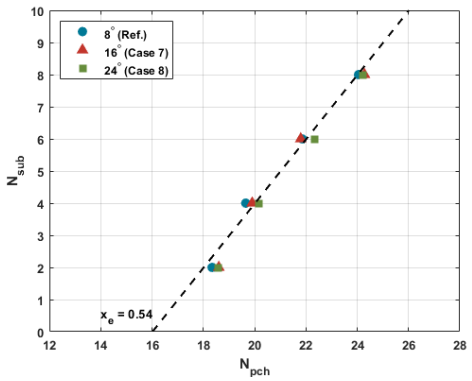

Fig. 8. Sensitivity to helix angle (Cases 7 and 8)

Figs. 9 through 12 illustrate the variation in total pressure drop for each case as heat power changes. It is noted that the arrow in each plot represents how much the pressure drop has changed when heat was increased. First, in examining Cases 1 and 2, it is evident that when $d_i = 9mm$, the change in total pressure drop is significantly larger (56 kPa vs. 11 kPa). When comparing Cases 3 and 4, it is apparent that the pressure drop is notably higher when $L = 35m$ (31 kPa vs. 14 kPa). These results imply a larger change in pressure drop increases the possibility of the system becoming relatively more unstable. However, in Fig. 11, the difference in the degree of change between cases is minimal (26 kPa vs. 21 kPa). Although the pressure drop is greater when the curvature ratio is small, the degree of change is almost similar to when the curvature ratio is large, indicating that the impact on DWO occurrence is nearly identical. In the case of the helical angle (Fig. 12), it is not a factor considered in the Colombo correlation, and while the pressure drop is relatively large when the helical angle is high due to gravity, the degree of change is similar for both helical angles.

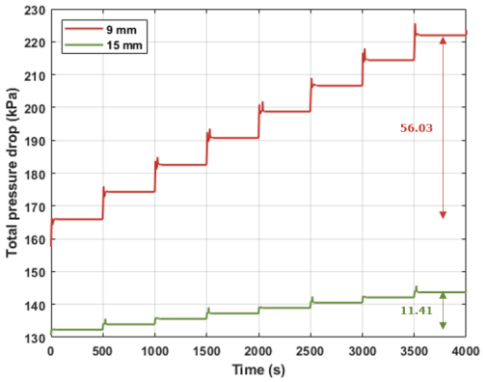

Fig. 9. Pressure drop change (Case 1 ($Q = 30\sim37kW$) Case 2 ($Q = 100\sim107kW$), $N_{sub} = 6$,)

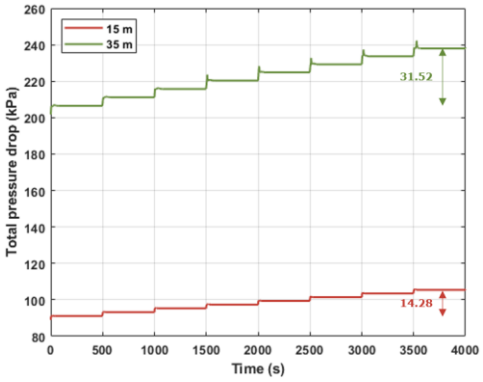

Fig. 10. Pressure drop change (Cases 3 and 4, $N_{sub} = 6$, $Q = 60\sim67kW$)

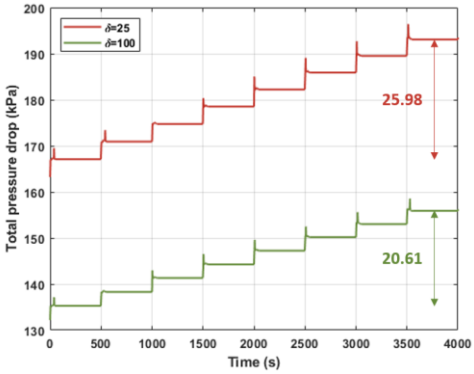

Fig. 11. Pressure drop change (Cases 5 and 6, $N_{sub} = 6$, $Q = 60\sim67kW$)

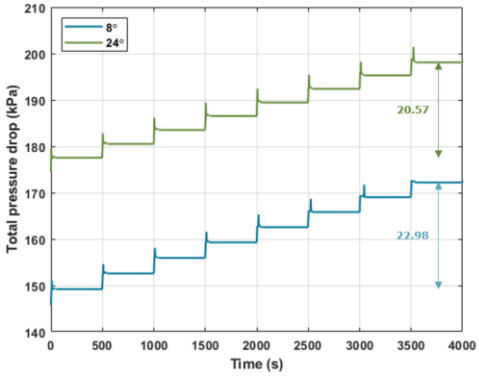

Fig. 12. Pressure drop change (Reference and Case 8, $N_{sub} = 6$, $Q = 60\sim67kW$)

4. Summary and Further Works

This study explored the sensitivity of various geometric parameters of HSG tubes to the onset of DWO using the modified MARS-KS code. The pressure drop correlations specific to helical tubes were newly added to the MARS-KS code. The findings indicate that the tube inner diameter and length significantly influence the onset of DWO. In contrast, the curvature ratio and helix angle were found to have minimal impact on DWO. This sensitivity may be due to using the correlation outside its valid range, resulting in similar pressure drop changes even when heat varied significantly.

Additionally, the previous experimental studies used helical tubes with identical geometries, leading to a lack of diverse experimental data. This limits the understanding of DWO and constrains the applicability of the MARS-KS code to advanced reactor designs. Future research should focus on experimental studies with varying geometric configurations to improve the reliability and applicability of the MARS-KS code in advanced reactors.

NOMENCLATURE

General symbols

h	Heat transfer coefficient (W/m^2K)
k	Thermal conductivity (W/mK)
d	Tube diameter (m)
D	Helical diameter (m)
Re	Reynolds number
Pr	Prandtl number
q''	Heat flux (W/m^2)
T	Temperature (K)
C_p	Specific heat capacity (J/kgK)
X_{tt}	Lockhart-Martinelli parameter
h_{fg}	Enthalpy difference between vapor saturation and liquid saturation
α	Void fraction

Greek symbols

ρ	Density (kg/m^3)
σ	Surface tension (N/m)
μ	Dynamic viscosity ($Pa\ s$)

Subscripts

mn	Mori-Nakayama
k	Liquid or Vapor
w	Wall
sat	Saturation
mic	Microscopic
NB	Nucleate boiling
TB	Transition boiling
f	Liquid
g	Vapor

ACKNOWLEDGEMENT

This work was supported by the Nuclear Safety Research Program through the Korea Foundation Of Nuclear Safety (KoFONS) using the financial resource granted by the Nuclear Safety and Security Commission (NSSC) of the Republic of Korea. (No. 00244146)

REFERENCES

[1] G. Yadigaroglu et al., An Experimental and Theoretical Study of Density-Wave Oscillations in Two-Phase Flow, HTL No. 74629-67, 1969.
[2] A. K. Nayak et al., Study on the stability behavior of two-phase natural circulation systems using a four-equation drift flux model, Nuclear Engineering and Design, Vol.237, 2007.
[3] D. Papini et al., Time-domain linear and non-linear studies on density wave oscillations, Chemical Engineering Science, Vol.81, 2012.
[4] D. Papini et al., Experimental and theoretical studies on density wave instabilities in helically coiled tubes, International Journal of Heat and Mass Transfer, Vol.68, 2014.
[5] M. Wang et al., Experimental and numerical studies on two-phase flow instability behavior of a parallel helically coiled system, Annals of Nuclear Energy, Vol.144, 2020.
[6] C. Shen et al., Study on two-phase flow instability of parallel helical tubes in steam generator of small modular reactors, International Communications in Heat and Mass Transfer, Vol.148, 2023.
[7] Seunghwan Oh et al., Exploring Two-Phase Flow Instabilities in Helical Steam Generators Using MARS-KS Code, Transactions of the Korean Nuclear Society Spring Meeting, 2024.
[8] KINS, MARS-KS CODE MANUAL Volume V: Models and Correlations Manual, KINS/RR-1822 Vol.5.
[9] H. Ito, Friction Factors for Turbulent Flow in Curved Pipes, Journal of Basic Engineering, 1959.
[10] M. Colombo et al., A scheme of correlation for frictional pressure drop in steam-water two-phase flow in helicoidal tubes, Chemical Engineering Science, Vol.123, 2015.
[11] L. Santini et al., Two-phase pressure drops in a helically coiled steam generator, International Journal of Heat and Mass Transfer, Vol.51, 2008.
[12] L. Zhao et al, Convective boiling heat transfer and two-phase flow characteristics inside a small horizontal helically coiled tubing once-through steam generator, International Journal of Heat and Mass Transfer, Vol.46, 2003.
[13] KAERI, Heat transfer test for the steam generator and PRHRS Heat Exchanger of SMART, KAERI/CM-1199/2009.
[14] KAERI, Methodology for Failure Assessment of SMART SG Tube with Once-through Helical-coiled type, KAERI/CM-1351/2010.
[15] M. Ishii et al., Thermally induced flow instabilities in two phase mixtures, International Heat Transfer Conference 4, 1970.